

## COMMUNICATION

[View Article Online](#)  
[View Journal](#) | [View Issue](#)

## Activation of $\text{CO}_2$ by $t\text{BuZnOH}$ species: efficient routes to novel nanomaterials based on zinc carbonates<sup>†</sup>

Cite this: *Chem. Commun.*, 2013, **49**, 5271

Received 4th March 2013,  
Accepted 18th April 2013

DOI: 10.1039/c3cc41639a

[www.rsc.org/chemcomm](http://www.rsc.org/chemcomm)

We report on the activation of  $\text{CO}_2$  by the well-defined alkylzinc hydroxide  $(t\text{BuZnOH})_6$  in the absence and presence of  $t\text{Bu}_2\text{Zn}$  as an external proton acceptor. The slight modifications in reaction systems involving organozinc precursors enable control of the reaction products with high selectivity leading to the isolation of the mesoporous solid based on  $\text{ZnCO}_3$  nanoparticles or an unprecedented discrete alkylzinc carbonate  $[(t\text{BuZn})_2(\mu_5\text{-CO}_3)]_6$  cluster with the Zn–C bond intact, respectively.

The chemical fixation and activation of  $\text{CO}_2$  has drawn long-standing interest as a means to mitigate global warming and utilize the captured  $\text{CO}_2$  as an inexpensive chemical feedstock.<sup>1,2</sup> Carbon dioxide is the most important and abundant C1-building block in Nature widely exploited by organisms (*i.e.* plants) for constructing larger carbohydrate-based building units. The most significant example of  $\text{CO}_2$  activation by zinc complexes is represented by carbonic anhydrase (CA), a zinc-metalloenzyme that catalyzes the reversible hydration of  $\text{CO}_2$  and is responsible for its fast metabolism.<sup>3</sup> This process is based on Zn–OH type reaction systems patterned on the active centre of CA. Hence, a number of mono- or dinuclear zinc complexes supported by multidentate ligands and featuring terminal or bridging hydroxide ligation have been widely investigated as synthetic analogues of CA.<sup>3–5</sup> However model studies mimicking the active Zn site in CA have so far failed to activate  $\text{CO}_2$  beyond the bicarbonate complex due to the product inhibition effect that has been commonly observed in these systems. Undoubtedly, it is of particular significance to gain experience from biochemical model systems and utilize the bio-inspired approach in the development of

more effective systems for  $\text{CO}_2$  fixation as well as in the construction of new functional materials based on metal carbonate cores. Surprisingly, the latter issues are still essentially an unexplored area,<sup>6</sup> and the use of well-defined alkylzinc compounds in this context is lacking.

The activation and conversion of  $\text{CO}_2$  into useful products has also long been recognized by organometallic chemists as a desirable goal. Nevertheless simple homoleptic zinc alkyls are known to be essentially inactive toward  $\text{CO}_2$ , due to the more covalent nature of the Zn–C bond in comparison to other M–C systems.<sup>1c</sup> The introduction of supporting ligands and the tuning of the zinc coordination sphere allow the enhancement of the reactivity of Zn complexes toward  $\text{CO}_2$  molecules. For example, the reaction of R–Zn–NR<sub>2</sub> compounds with  $\text{CO}_2$  yields zinc-carbamates<sup>7</sup> while the insertion of  $\text{CO}_2$  into Zn–OR is a basic step in the alternating copolymerization of  $\text{CO}_2$  with epoxides.<sup>8</sup> In this regard, organozinc RZnOH-type compounds appear as very attractive model reagents due to the presence of both the  $\text{CO}_2$ -reactive ZnOH group and the proton-reactive Zn–C bond (Scheme 1a) in their structure. However, low-alkyl RZnOH compounds are fairly unstable<sup>9</sup> and only recently our group provided a well-defined alkylzinc hydroxide, *i.e.*  $[t\text{BuZnOH}]_6$  (**1**) (Scheme 1b).<sup>10</sup>

Herein we report on the activation of  $\text{CO}_2$  by **1** in the absence as well as in the presence of  $t\text{Bu}_2\text{Zn}$  as a proton acceptor. We demonstrate that the reaction of **1** with  $\text{CO}_2$  affords the unprecedented mesoporous material **2** based on  $\text{ZnCO}_3$  nanoparticles of uniform size and shape, whereas  $t\text{Bu}_2\text{Zn}$  promotes the formation of the unique discrete dodecanuclear alkylzinc carbonate cluster  $[(t\text{BuZn})_2(\mu_5\text{-CO}_3)]_6$  (**3**).

The exposure of the freshly dissolved alkylzinc hydroxide **1** in toluene to a dry and oxygen-free  $\text{CO}_2$  atmosphere at room

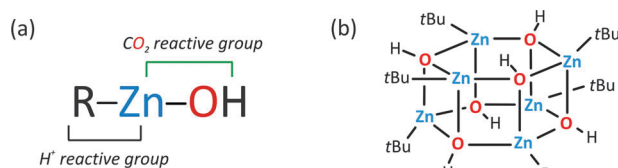
<sup>a</sup> Institute of Physical Chemistry, Polish Academy of Sciences, Kasprzaka 44/52, 01-224 Warsaw, Poland

<sup>b</sup> Faculty of Chemistry, Warsaw University of Technology, Noakowskiego 3, 00-664 Warsaw, Poland. E-mail: lewin@ch.pw.edu.pl;

Web: <http://lewin.ch.pw.edu.pl/>; Fax: +48-22-234-7279

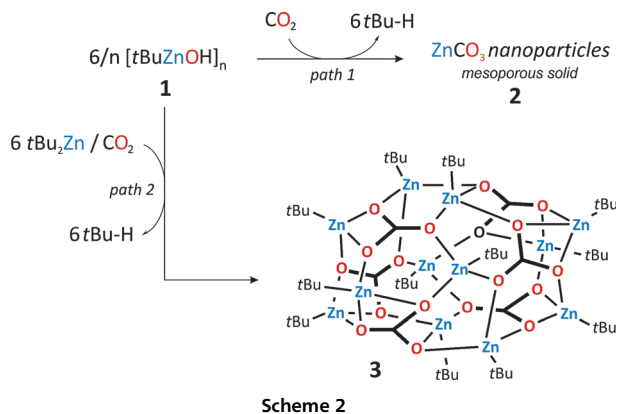
<sup>c</sup> Institute of High Pressure Physics Unipress, Polish Academy of Sciences, Sokolowska 29/37, 01-142 Warsaw, Poland

<sup>†</sup> Electronic supplementary information (ESI) available: Full experimental details for **2** and **3** including experimental procedures, analytical data, X-ray and spectroscopic data. CCDC 866665 (3). For ESI and crystallographic data in CIF or other electronic format see DOI: 10.1039/c3cc41639a



**Scheme 1** (a) Presentation of reactive species in an RZnOH type compound and (b) representative alkylzinc hydroxide **1**.





temperature afforded repeatedly the formation of a gel of zinc carbonate nanoparticles **2** (Scheme 2, path 1). After more detailed investigations we found that an excess of *t*Bu<sub>2</sub>Zn in the system involving **1** and CO<sub>2</sub> shifts the reaction course to the unprecedented dodecanuclear alkylzinc carbonate cluster  $[(t\text{BuZn})_2(\mu_5\text{-CO}_3)]_6$  (**3**) with a moderate yield (isolated yield 38% for *t*BuZnOH:*t*Bu<sub>2</sub>Zn molar ratio 2:1), while the equimolar mixture of **1** and *t*Bu<sub>2</sub>Zn in toluene as a starting reaction system leads to the formation of **3** almost quantitatively (isolated yield 91%; Scheme 2, path 2).

The resulting zinc carbonate **2** in the form of a white gel (gelation of the post-reaction mixture occurs within 24 h), upon aging for two weeks under ambient conditions, transforms into a suspension of solid, which can be separated by decantation. The latter solid **2** with the bulk density as low as 0.24 g cm<sup>-3</sup>, representing 5.4% of the density of a single crystal of ZnCO<sub>3</sub> (4.44 g cm<sup>-3</sup>), was characterized using scanning (SEM) and transmission (TEM) electron microscopy as well as infrared (IR) spectroscopy and elemental analysis. The SEM micrographs show the macro- (>50 nm) and mesoporous (2–50 nm) character of the described material **2** (Fig. 1a).

The TEM micrographs of **2** show that the material consists of an interconnected network of essentially spherical

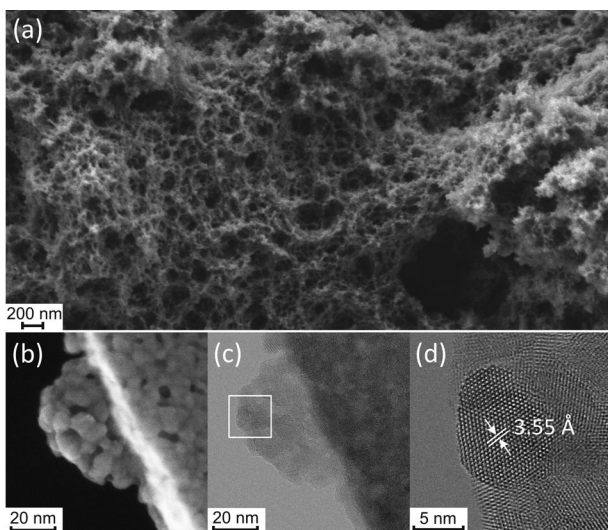


**Fig. 1** Images of the mesoporous solid **2**: (a) SEM image showing meso- and macro-pores; (b) STEM image showing nanosized pores; (c) the same fragment in TEM mode; (d) HRTEM image of a single particle showing the crystalline nature of the nanoparticle architecture (lattice fringes corresponding to the (102) reflections of trigonal ZnCO<sub>3</sub>).

(mean diameter of 8.0 nm) ZnCO<sub>3</sub> nanoparticles (Fig. 1b–d) as indicated by interplanar distances (*d*-values), 3.55 Å (±0.05) corresponding to the *d*-values of (102) planes of ZnCO<sub>3</sub> (Fig. 1d). The porosity of **2** was verified by N<sub>2</sub> adsorption at 77 K. Compound **2** adsorbs N<sub>2</sub> with a maximum uptake of 250 cm<sup>3</sup> g<sup>-1</sup> and exhibits a type IV isotherm characteristic for mesoporous materials [Fig. S3 in the ESI†]. The calculated Brunauer–Emmett–Teller (BET) surface area for **2** is 91 m<sup>2</sup> g<sup>-1</sup> and Barrett–Joyner–Halenda (BJH) analysis shows that the average pore diameter falls in the range of 7–15 nm, which is a commonly observed value for xero- and aerogels of many semiconductors.<sup>11c–f</sup> It is worth noting that the majority of known aerogels contain silica as the inorganic matrix and the development of this type of material based on other inorganic building blocks is still at an early stage.<sup>11</sup>

In contrast to the **1**–CO<sub>2</sub> system, the reaction in the presence of an equimolar amount of *t*Bu<sub>2</sub>Zn leads to the alkylzinc carbonate **3**. Compound **3** is stable at ambient temperature under an inert atmosphere in the solid state as well as in solution. The presence of the carbonate group in **3** is indicated by a singlet resonance at 165.3 ppm in the CP-MAS <sup>13</sup>C NMR spectrum as well as by a strong band at 1510 cm<sup>-1</sup> in the IR spectrum (Fig. S4 and S5 in the ESI†).<sup>6a</sup> Crystallization from a dilute toluene solution at 25 °C afforded colourless cubic crystals of **3** suitable for X-ray single-crystal determination.

Compound **3** crystallizes in the trigonal space group *R*3̄ as a dodecanuclear cluster  $[(t\text{BuZn})_2(\mu_5\text{-CO}_3)]_6$ , which is an unprecedented alkylzinc carbonate aggregate (Fig. 2a). The association of six  $(t\text{BuZn})_2\text{CO}_3$  units in **3** results in a nanometer-sized barrel-like structure (*ca.* 17.0 × 14.0 Å) of fused networks of four- and six-membered heterocycles. Each carbonate anion acts as a bridging as well as a chelating ligand and bridges five zinc centres adopting the  $\eta^2\text{:}\eta^2\text{:}\eta^2\text{:}\mu_5$  coordination mode, which is very rare for carbonate–metal complexes<sup>12,13</sup> and has not been reported for zinc compounds so far (Fig. 2b). The trigonal geometry of carbonate ligands is slightly distorted, which is expressed by a range of the O–C–O angles [116°–122°] as well as the C–O bonds lengths (1.279–1.295 Å) (Fig. 2b). The central core of **3** is comprised of six four-coordinate zinc atoms bridged by six carbonate moieties, which form a hexagonal cage ( $\text{ZnCO}_3$ )<sub>6</sub> with faces built of six-membered rings in which the Zn–O bond lengths fall within a range of 2.067–2.218 Å. Interestingly, the core in **3** is very similar to a structural motif of the hexameric ethylzinc benzoate complex,<sup>14</sup> and the related methylzinc derivative of *N*-methyl benzamide,<sup>15</sup> however, it is further extended on both brims by additional three *t*BuZn moieties at each side, forming six-membered (Zn–O)<sub>3</sub> rings representing a highly puckered chair-like conformation. The Zn–O distances are of two types, those bridging [2.067–2.102 Å] and those chelating [2.102–2.218 Å] zinc centers. The crystal structure of **3** is based on close-packing of molecules in a hexagonal arrangement with linear ordered molecules along the *c* axis (see Fig. S2 in the ESI†). Notably, to date there have been only a few examples of structurally characterized high nuclearity zinc clusters, which are regarded as potential SBU units for materials chemistry.<sup>16</sup>

In conclusion, we have demonstrated for the first time that the alkylzinc hydroxides can be successfully utilized for the activation of CO<sub>2</sub> under mild conditions. Just by a slight modification of the reaction systems we isolated a mesoporous



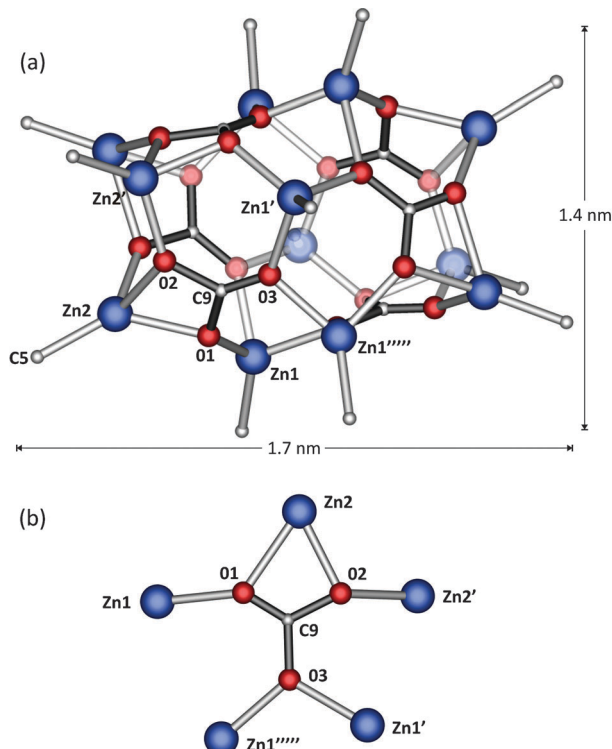


**Fig. 2** (a) Molecular structure of **3**; methyl groups of *tert*-butyl groups have been omitted for clarity; selected bond lengths (Å) and angles (deg): Zn1–C1, 1.973(4); Zn1–O1, 2.067(2); Zn2–O1, 2.102(2); C9–O1, 1.295(4); C9–O2, 1.279(4); C9–O3, 1.279(4); O1–C9–O2, 116.4(3); O1–C9–O3, 120.8(3); O2–C9–O3, 122.8(3); Zn1–O1–Zn2, 109.7(1); C9–O1–Zn1, 132.2(2); C9–O1–Zn2, 93.4(2); and (b) view of the coordination mode of the carbonate anion in **3**.

solid **2** based on single  $\text{ZnCO}_3$  nanoparticles or the unprecedented dodecanuclear alkylzinc carbonate complex  $[(t\text{BuZn})_2(\mu_5\text{-CO}_3)]_6$  (**3**). Thus, alkylzinc hydroxides appear to be interesting examples of organometallic  $\text{Zn}-\text{OH}$ -type compounds with reactive  $\text{Zn}-\text{C}$  bonds, where both functionalities can take part in sequential transformations. We believe that this approach shows the unique potential of simple organometallic precursors for post-synthetic modifications in order to design new functional materials based on biocompatible zinc carbonate components. Further studies on the effective fixation of  $\text{CO}_2$  and other small molecules by organozinc hydroxides supported by organic ligands are in progress.

The authors would like to acknowledge the National Science Centre (Grant UMO-2011/01/N/ST5/05562, K.S.) and the Foundation for Polish Science Team Programme co-financed by the European Regional Development Fund Grant No. TEAM/2011-7/8 (J.L., I.J., M.W.) for financial support. We are grateful to Dr J. Grzonka for TEM measurements.

## Notes and references

1 (a) *Carbon dioxide as chemical feedstock*, ed. M. Aresta, Wiley-VCH, Weinheim, 2010; (b) G. A. Olah, G. K. S. Prakash and A. Goeppert, *J. Am. Chem. Soc.*, 2011, **133**, 12881–12898; (c) M. Cokoja, C. Bruckmeier, B. Rieger, W. A. Herrmann and F. E. Kühn, *Angew. Chem., Int. Ed.*, 2011, **50**, 8510–8537; (d) M. Mikkelsen, M. Jørgensen and F. C. Krebs, *Energy Environ. Sci.*, 2010, **3**, 43–81; (e) T. Sakakura, J.-C. Choi and H. Yasuda, *Chem. Rev.*, 2007, **107**, 2365–2387;

(f) H. Arakawa, M. Aresta, J. N. Armor, M. A. Bartea, E. J. Beckman, A. T. Bell, J. E. Bercaw, C. Creutz, E. Dinjus, D. A. Dixon, K. Domen, D. DuBois, J. Leckert, E. Fujita, D. H. Gibson, W. A. Goddard, D. W. Goodman, J. Keller, G. J. Kubas, H. H. Kung, J. E. Lyons, L. E. Manzer, T. J. Marks, K. Morokuma, K. M. Nicholas, R. Periana, L. Que, J. Rostrup-Nielsen, W. M. H. Sachtler, L. D. Schmidt, A. Sen, G. A. Somorjai, P. C. Stair, B. R. Stults and W. Tumas, *Chem. Rev.*, 2001, **101**, 953–996.

2 (a) C. Finn, S. Schnittger, L. J. Yellowlees and J. B. Love, *Chem. Commun.*, 2012, **48**, 1392–1399; (b) A. Decortes, A. M. Castilla and W. A. Kleij, *Angew. Chem., Int. Ed.*, 2010, **51**, 9822–9837; (c) E. E. Benson, C. P. Kubiak, A. J. Sathrum and J. M. Smieja, *Chem. Soc. Rev.*, 2009, **38**, 89–99.

3 V. M. Krishnamurthy, G. K. Kaufman, A. R. Urbach, I. Gitlin, K. L. Gudiksen, D. B. Weibel and G. M. Whitesides, *Chem. Rev.*, 2008, **108**, 946–1051.

4 (a) H. Vahrenkamp, *Dalton Trans.*, 2007, 4751–4759; (b) G. Parkin, *Chem. Rev.*, 2004, **104**, 699–767; (c) H. Vahrenkamp, *Acc. Chem. Res.*, 1999, **32**, 589–596.

5 For selected examples, see: (a) W. Sattler and G. Parkin, *Chem. Sci.*, 2012, **3**, 2015–2019; (b) D. Huang, O. V. Makhlynets, L. L. Tan, S. C. Lee, E. V. Rybak-Akimova and R. H. Holm, *Proc. Natl. Acad. Sci. U. S. A.*, 2011, **108**, 1222–1227; (c) H. Brombacher and H. Vahrenkamp, *Inorg. Chem.*, 2004, **43**, 6042–6049; (d) C. Bergquist, T. Fillebeen, M. M. Morlok and G. Parkin, *J. Am. Chem. Soc.*, 2003, **125**, 6189–6199; (e) L. Cronin and P. H. Walton, *Chem. Commun.*, 2003, 1572–1573; (f) M. Rombach, H. Brombacher and H. Vahrenkamp, *Eur. J. Inorg. Chem.*, 2002, 153–159; (g) C. Bergquist and G. Parkin, *J. Am. Chem. Soc.*, 1999, **121**, 6322–6323; (h) S. Hikichi, M. Tanaka and Y. Moro-oka, *J. Am. Chem. Soc.*, 1993, **115**, 5496–5508; (i) A. Looney, R. Han, K. McNeill and G. Parkin, *J. Am. Chem. Soc.*, 1993, **115**, 4690–4697; (j) E. Kimura, T. Shiota, T. Koike, M. Shiro and M. Kodama, *J. Am. Chem. Soc.*, 1990, **112**, 5805–5811.

6 (a) S. I. Swamy, J. Bacsa, J. T. A. Jones, K. C. Stylianou, A. Steiner, L. K. K. Ritchie, T. Hasell, J. A. Gould, A. Laybourn, Y. Z. Khimyak, D. J. Adams, M. J. Rosseinsky and A. I. Cooper, *J. Am. Chem. Soc.*, 2010, **132**, 12773–12775; (b) B. F. Abrahams, A. Hawley, M. G. Haywood, T. A. Hudson, R. Robson and D. A. Slizys, *J. Am. Chem. Soc.*, 2004, **126**, 2894–2904; (c) A. Company, J.-E. Jee, X. Ribas, J. M. Lopez-Valbuena, L. Gomez, M. Corbella, A. Llobet, J. Mahia, J. Benet-Buchholtz, M. Costas and R. van Eldik, *Inorg. Chem.*, 2007, **46**, 9098–9110.

7 For example see: Y. Tang, W. S. Kassel, L. N. Zakharov, A. L. Rheingold and R. A. Kemp, *Inorg. Chem.*, 2005, **44**, 359–364.

8 (a) D. J. Daresbourg, *Chem. Rev.*, 2007, **107**, 2388–2410; (b) G. W. Coates and D. R. Moore, *Angew. Chem.*, 2004, **116**, 6784–6806 (*Angew. Chem., Int. Ed.*, 2004, **43**, 6618–6639).

9 W. Kuran and M. Czarnecka, *J. Organomet. Chem.*, 1984, **263**, 1–7.

10 W. Bury, E. Krajewska, M. Dutkiewicz, K. Sokołowski, I. Justyniak, Z. Kaszkur, K. J. Kurzydłowski, T. Płociński and J. Lewiński, *Chem. Commun.*, 2011, **47**, 5467–5469.

11 For selected examples of metal chalcogenides based aerogels see: (a) J. Yuan, D. Wen, N. Gaponik and A. Eychmüller, *Angew. Chem., Int. Ed.*, 2013, **52**, 976–979; (b) M. Krumm, C. L. Pueyo and S. Polarz, *Chem. Mater.*, 2010, **22**, 5129–5136; (c) I. U. Arachchige and S. L. Brock, *Acc. Chem. Res.*, 2007, **40**, 801–809; (d) I. U. Arachchige and S. L. Brock, *J. Am. Chem. Soc.*, 2006, **128**, 7964–7971; (e) J. L. Mohanan, I. U. Arachchige and S. L. Brock, *Science*, 2005, **307**, 397–401; (f) A. C. Pierre and G. M. Pajonk, *Chem. Rev.*, 2002, **102**, 4243–4265.

12 D. A. Palmer and R. van Eldik, *Chem. Rev.*, 1983, **83**, 651–731.

13 A. N. Acharya, A. Das and A. C. Dash, *Adv. Inorg. Chem.*, 2004, **55**, 127–199.

14 J. Lewiński, W. Bury, M. Dutkiewicz, M. Maurin, I. Justyniak and J. Lipkowska, *Angew. Chem., Int. Ed.*, 2008, **47**, 573–576.

15 S. R. Boss, R. Haigh, D. J. Linton, P. Schooler, G. P. Shields and A. E. H. Wheatley, *Dalton Trans.*, 2003, 1001–1008.

16 For selected examples, see: (a) A. Muller, B. Neumuller and K. Dehnicke, *Angew. Chem., Int. Ed. Engl.*, 1997, **36**, 2350; (b) Y. Yang, J. Pinkas, M. Noltemeyer, H.-G. Schmidt and H. W. Roesky, *Angew. Chem., Int. Ed.*, 1999, **38**, 664–666; (c) R. Boomishankar, P. I. Richards and A. Steiner, *Angew. Chem., Int. Ed.*, 2006, **45**, 4632–4634; (d) T. Cadenbach, T. Bollermann, C. Gemel, I. Fernandez, M. von Hopffgarten, G. Frenking and R. A. Fischer, *Angew. Chem., Int. Ed.*, 2008, **47**, 9150–9154; (e) T. Cadenbach, T. Bollermann, C. Gemel, M. Tombul, I. Fernandez, M. von Hopffgarten, G. Frenking and R. A. Fischer, *J. Am. Chem. Soc.*, 2009, **131**, 16063–16077.

